



Article

Green Catalytic Conversion of Some Benzylic Alcohols to Acids by NiO₂ Nanoparticles (NPNPs) in Water

Abdel Ghany F. Shoair^{1,2,*}, Mai M. A. H. Shanab³, Nasser A. El-Ghamaz⁴, Mortaga M. Abou-Krishna^{5,6},
Sayed H. Kenawy^{6,7} and Tarek A. Yousef^{6,8}

- ¹ Department of Science and Technology, University College-Ranyah, Taif University, Taif 21975, Saudi Arabia
² High Altitude Research Center, Taif University, Taif 21975, Saudi Arabia
³ Department of Chemistry, College of Sciences and Humanities Studies (Girls Section), Hawtat Bani Tamim, Prince Sattam Bin Abdulaziz University, Al-Kharj 11149, Saudi Arabia; m.hassan@psau.edu.sa
⁴ Department of Physics, Faculty of Science, Damietta University, New Damietta 34517, Egypt; elghamaz@du.edu.eg
⁵ Faculty of Science, Chemistry Department, South Valley University, Qena 83523, Egypt; mmaboukrisha@imamu.edu.sa
⁶ Chemistry Department, College of Science, Imam Mohammad Ibn Saud Islamic University (IMSIU), Riyadh 11623, Saudi Arabia; skibrahim@imamu.edu.sa (S.H.K.); tayousef@imamu.edu.sa (T.A.Y.)
⁷ Refractories, Ceramics and Building Materials Department, National Research Centre, El-Buhouth St., Dokki, Giza 12622, Egypt
⁸ Toxic and Narcotic Drugs Laboratory, Department of Forensic Medicine, Mansoura Laboratory, Medico Legal Organization, Ministry of Justice, Mansoura 35516, Egypt
* Correspondence: afshaair@tu.edu.sa

Abstract: The aqueous basic systems NiSO₄·6H₂O/K₂S₂O₈ (pH = 14) and NiSO₄·6H₂O/KBrO₃ (pH = 11.5) were investigated for the catalytic conversion of benzyl alcohol and some para-substituted benzyl alcohols to their corresponding acids in 75–97% yields at room temperature. The active species was isolated and characterized using scanning electron microscopy (SEM), transmission electron microscopy (TEM), X-ray powder diffraction, EDX and FT-IR techniques, and identified as comprising NiO₂ nanoparticles (NPNPs). The SEM and TEM images of the Ni peroxide samples showed a fine spherical-like aggregation of NiO₂ molecules with a nearly homogeneous partial size and confirmed the aggregation's size to be in the range of 2–3 nm. The yields, turn over (TO) and turn over frequencies (TOF) were calculated. It was noticed that the aromatic alcohols containing para-substituted electron donation groups gave better yields than those having electron withdrawing groups. The optimum conditions for this catalytic reaction were studied using benzyl alcohol as a model. The mechanism of the catalytic conversion reaction was suggested, in which the produced NPNPs convert alcohols to acids in two steps through the formation of the corresponding aldehyde. The produced NiO because of this conversion is converted again to NPNPs by the excess of K₂S₂O₈ or KBrO₃. This catalytic cycle continues until all of the substrate is oxidized.

Keywords: nickel peroxide nanoparticles (NPBPs); catalyst; benzyl alcohol; green oxidation



Citation: Shoair, A.G.F.; Shanab, M.M.A.H.; El-Ghamaz, N.A.; Abou-Krishna, M.M.; Kenawy, S.H.; Yousef, T.A. Green Catalytic Conversion of Some Benzylic Alcohols to Acids by NiO₂ Nanoparticles (NPNPs) in Water. *Catalysts* **2023**, *13*, 645. <https://doi.org/10.3390/catal13040645>

Academic Editors: Ana Maria Faisca Phillips, Elisabete C.B.A. Alegria and Luísa Margarida Martins

Received: 25 February 2023

Revised: 17 March 2023

Accepted: 18 March 2023

Published: 23 March 2023



Copyright: © 2023 by the authors. Licensee MDPI, Basel, Switzerland. This article is an open access article distributed under the terms and conditions of the Creative Commons Attribution (CC BY) license (<https://creativecommons.org/licenses/by/4.0/>).

1. Introduction

The green protocol for the production of valuable chemicals is of great significance in the sustainable development of green economy [1]. The oxidation of benzyl alcohols to aromatic acids using green routes is very important to avoid bad effects on the environment [2]. The production of aromatic acids is important in organic synthesis, since it is used as an intermediate in the synthesis of many fine chemicals such as drugs and vitamins [3]. The use of stoichiometric amounts of inorganic transition metal salts such as copper (I) [4], copper(II) [5] permanganate [6], chromium(VI) [7] and iron(III) [8,9] is often toxic and generates a considerable amount of by-product. The use of precious metals such as Pt [10], Pd [11] and Ru [12] is industrially restricted due to their high cost and

scarcity. The extremely small size of nanoparticles enlarges the surface area and allows more reactions to occur, displaying high catalytic activity [13–17]. Recently, benzoic acid was synthesized via the pyrolysis of xylan to toluene followed by the subsequent catalytic oxidation of toluene to benzoic acid by the bimetallic catalyst $\text{Co}_2\text{MnO}_4@\text{MCM-41}$ [18]. Oroujzadeh et al. [19] reported the catalytic oxidation of benzyl alcohol to benzoic acid by the $[\text{CuClL}_2]$ ($\text{L} = \text{N-nicotinyl}; \text{N-N''-bis(tert-butyl) phosphoric triamide}$) complex at 78°C in aceto-nitrile as a solvent. A mixture of benzaldehyde and benzoic acid was obtained from the catalytic oxidation of benzyl alcohol by the potassium salt of the Keggin heteropolyacids $\text{K}_5\text{PW}_{11}\text{NiO}_{39}$ in the presence of H_2O_2 [20]. To the best of my knowledge, few reports have been on for the applications of nickel peroxide in the catalytic oxidation of organic compounds. Goerge et al. reported a good review on the use of nickel peroxide for the oxidation of many organic compounds, including alcohols, phenols and amines [21]. The synthesis of diacetone-2-ketoL-gulonic acid, an intermediate in the synthesis of vitamin C, was reported by Weijlard via the addition of nickel salts in a solution of sodium hypochlorite [22]. Nakgawa et al. reported on the use of an aqueous solution of nickel-sulfate-treated sodium hypochlorite in an alkaline medium for the stoichiometric oxidation of primary alcohols to their corresponding acids and to their corresponding carbonyl compounds in an organic solvent [23], and also on the synthesis of 2-phenylbenzoxazoles from their corresponding Schiff bases [24,25]. As part of our ongoing interest in the catalytic oxidation of organic compounds by transition metal–oxo complexes [26], we decided to study the catalytic oxidation of a number of aromatic alcohols to their corresponding acids catalyzed by the reagent $\text{NiSO}_4 \cdot 6\text{H}_2\text{O}/\text{K}_2\text{S}_2\text{O}_8$ or KBrO_3 in an aqueous basic medium. A number of factors were studied to optimize the reaction conditions. The active species was isolated and characterized as comprising nickel peroxide nanoparticles (NPNPs). A plausible mechanism for this catalytic reaction was suggested.

2. Results and Discussion

2.1. Synthesis of the Catalyst

The nickel peroxide nanoparticles were synthesized using the co-precipitation method by mixing two equal amounts of nickel sulfate and potassium persulfate in the presence of four equivalent parts of KOH in water according to Equation (1):



$\text{K}_2\text{S}_2\text{O}_8$ and KBrO_3 act as co-oxidants and react with $\text{NiSO}_4 \cdot 6\text{H}_2\text{O}$ in the presence of KOH as a basic medium to generate NiO_2 , for example in Equation (1). The black nickel peroxide NPNPs were filtered, washed with H_2O and dried at 60°C for three hours.

2.2. Characterization of Nickel Peroxide Nanoparticles (NPNPs)

2.2.1. FTIR Spectrum of NiO_2 Nanoparticles (NPNPs)

The FT-IR spectrum showed several significant absorption peaks (Figure 1). The absorption bands in the range of $500\text{--}550\text{ cm}^{-1}$ were assigned to the NiO stretching vibrational mode [27,28]. The weak absorption band at around 720 cm^{-1} is characteristic of the peroxo O–O stretching vibrational mode [29]. It was noticed that a broad absorption band and a weak band at 3405 cm^{-1} and 1630 cm^{-1} were attributable to O–H and H–O–H bending and stretching vibrational modes, respectively [30].

These bands were due to the hydration of the FTIR sample disk when it was prepared in open air. Other bands were observed in the range of $1070\text{--}1450\text{ cm}^{-1}$; these bands were assigned to the absorbed carbon dioxide by the sample disk [31].

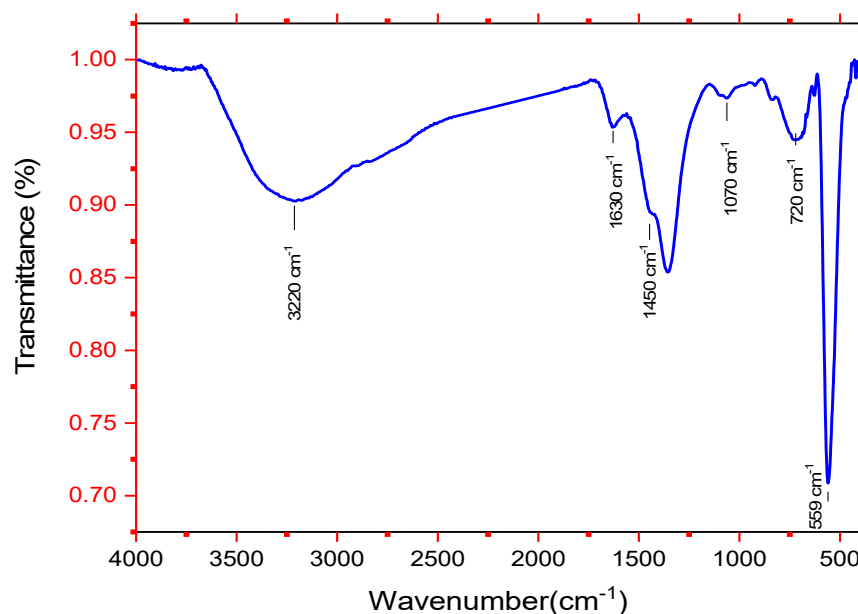


Figure 1. Vibrational Fourier transform infrared (FT-IR) spectrum of the NiO₂ nanoparticles (NPNPs).

2.2.2. EDX Analysis

The stoichiometry of the as-synthesized Ni peroxide (NiO₂) powder was examined using energy-dispersive spectroscopy (EDS), as shown in Figure 2. The atomic weight ration of nickel to oxygen (Ni/O) was found to be 1.96, which was in good agreement with the theoretically calculated value of 1.83 [32]. The results reported by Kooti et al. [28] showed that the experimental obtained values of Ni/O were 1.73 and 3.67 for NiO₂ and NiO, respectively. The present results extracted from the EDS confirmed the good stoichiometry of the prepared Ni peroxide.

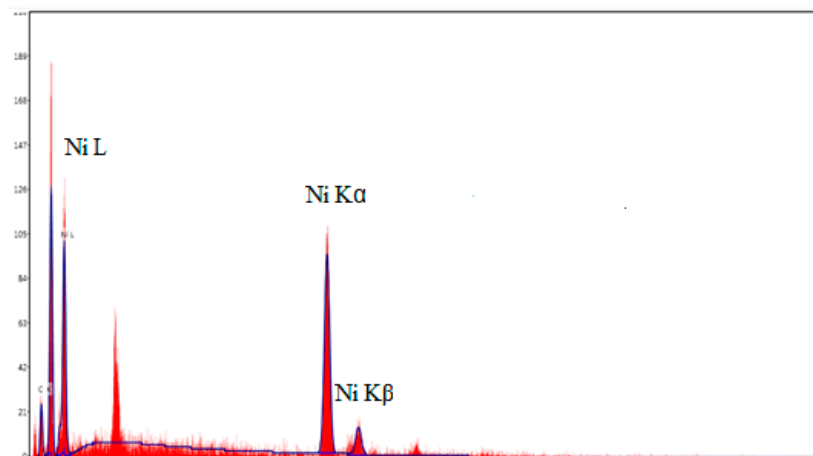


Figure 2. EDX spectrum of NiO₂ nanoparticles (NPNPs).

2.2.3. XRD Analysis

The XRD pattern of the NiO₂ powder is shown in Figure 3. The two broad peaks around $2\theta \sim 17.6^\circ$ and 37.2° with the superimposed sharp peaks indicate polycrystalline ultra-nano-sized particles of NiO₂. The peaks positioned at $2\theta \approx 37.8^\circ$ and 43.9° can be assigned to the (111) and (200) crystal planes, respectively, (JCPDS 47-1049) [33]. The average crystallite size of the NiO₂ powder under investigation was found to be 1.3 nm. The obtained average crystallite size suggests the synthesized NiO₂ to comprise ultra-small nanoparticles. Earlier, Seguin et al. [32] reported and confirmed the monoclinic crystal

system of NiO₂. The average crystallite size (L) of NiO₂ powder can be estimated by employing the following Sherrer's equation [33–35]:

$$L = \frac{k\lambda}{\beta \cos(\theta)}$$

where $k = 0.95$ is the wavelength of the used X-ray, θ is the full width at half maximum of the diffraction peak measured in radians, and θ is the Bragg's angle.

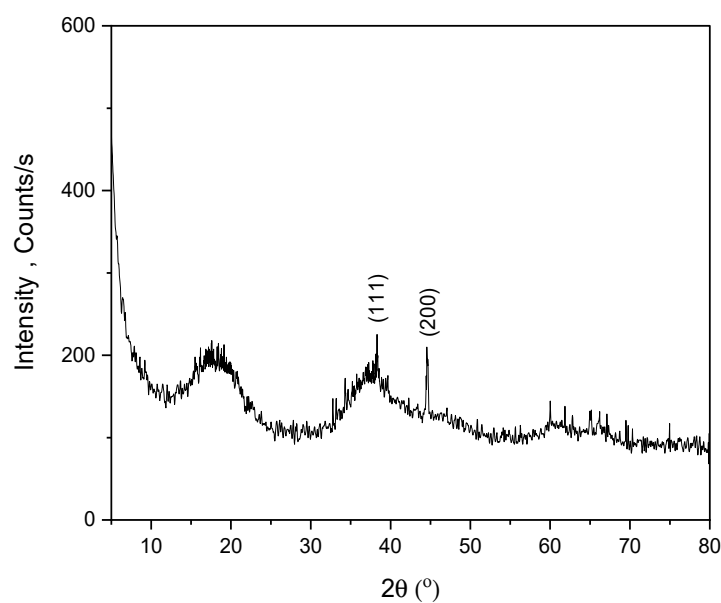


Figure 3. Powder X-ray diffraction (XRD) results for the NiO₂ nanoparticles (NPNPs).

2.3. SEM and TEM

The SEM images of NiO₂ samples are presented in Figure 4a,b. The SEM image in Figure 4a shows fine spherical-like aggregations of NiO₂ molecules with a nearly homogeneous particle size. The TEM image in Figure 4b confirms the aggregations' size to be in the range of 2–3 nm. This result confirms the ultra-small size of the NiO₂ nanoparticles obtained using Sherrer's equation. On the other hand, the electron diffraction pattern (EDP) in the inset of Figure 4b confirms the fine-sized polycrystalline phase of the NiO₂.

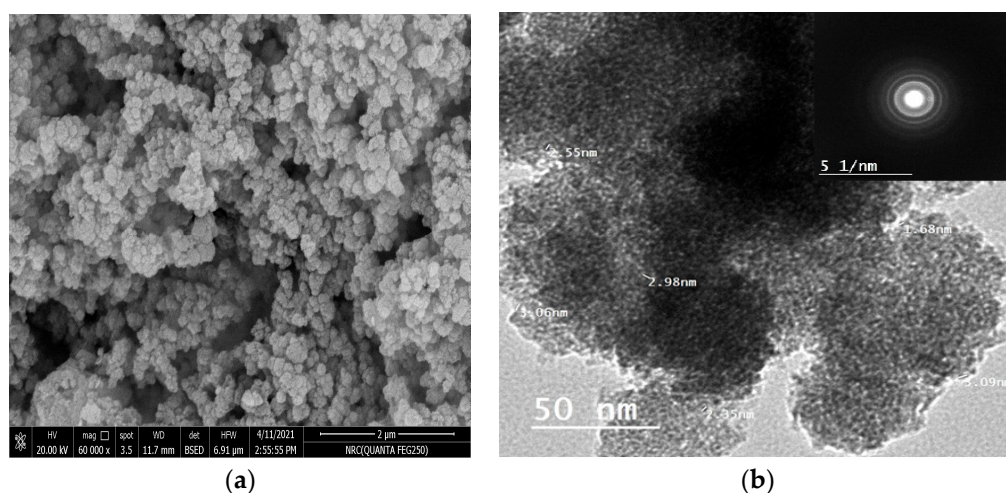
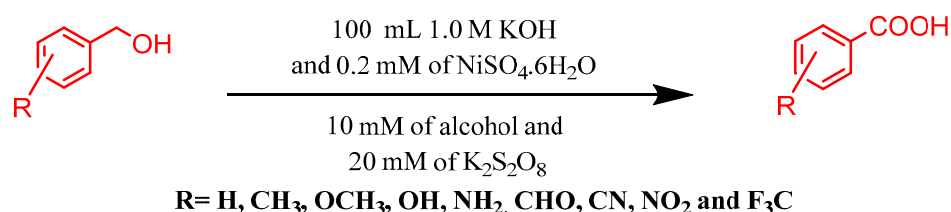


Figure 4. (a) SEM image of the NPNPs and (b) TEM images of the NiO₂ nanoparticles (NPNPs).

2.4. Catalytic Oxidation of Alcohols

We decided to investigate the catalytic activity of nickel peroxide nanoparticles (NPNPs) generated in situ from nickel salts such as $\text{NiSO}_4 \cdot 6\text{H}_2\text{O}$, $\text{NiCl}_2 \cdot 6\text{H}_2\text{O}$, and $\text{Ni}(\text{CH}_3\text{COO})_2 \cdot 2\text{H}_2\text{O}$ in the presence of $\text{K}_2\text{S}_2\text{O}_8$ in 1.0 M aqueous KOH or KBrO_3 in 1.0 M aqueous K_2CO_3 for the catalytic conversion of benzyl alcohol and some *p*-substituted benzyl alcohols containing electron-withdrawing and electron-donating groups to their corresponding acids. Additionally, we also investigated the optimum conditions for conducting this catalytic reaction (Scheme 1).



Scheme 1. Catalytic oxidation of benzyl alcohol and some *p*-substituted benzyl alcohol by $\text{NiSO}_4 \cdot 6\text{H}_2\text{O}/\text{K}_2\text{S}_2\text{O}_8$.

Benzyl alcohol was selected as a model substrate of $\text{NiSO}_4 \cdot 6\text{H}_2\text{O}$ for the in situ generation of nickel peroxide nanoparticles (NPNPs), which were the active catalytic species in this reaction, with two co-oxidants $\text{K}_2\text{S}_2\text{O}_8$ in 1.0 M KOH (pH = 14) and KBrO_3 in 1.0 M K_2CO_3 (pH = 11.5) as co-oxidants.

A set of experiments were carried out using two different nickel salts instead of $\text{NiSO}_4 \cdot 6\text{H}_2\text{O}$ with two different co-oxidants additionally, and two experiments were performed at 50 °C and 80 °C. The results are presented in Table 1.

It was found that the oxidation of benzyl alcohol (10 mM) to the corresponding benzoic acid took place smoothly in a short time (4 h) with the use of 0.2 mM of $\text{NiSO}_4 \cdot 6\text{H}_2\text{O}$ (50 fold-excess of the substrate) and 20 mM of the co-oxidants (two fold-excess of the substrate) in 100 mL of aqueous KOH (1.0 M). These conditions gave 97% and 75% benzoic acid with $\text{K}_2\text{S}_2\text{O}_8$ and KBrO_3 as the co-oxidants, respectively, at ambient temperature (entry 1, Table 1). The yields obtained with KBrO_3 in 1.0 M K_2CO_3 (pH = 11.5) were lower than those obtained with $\text{K}_2\text{S}_2\text{O}_8$ in 1.0 M KOH (pH = 14), which was probably due to $\text{K}_2\text{S}_2\text{O}_8$ having a stronger oxidizing power and higher aqueous solubility and stability suitable for the formation of the active species (NPNPs) than KBrO_3 .

When we conducted two reactions at 50 °C and 80 °C, respectively, the yields of the benzoic acid were lower than those obtained at ambient temperature and the reaction was smelly with the formation of unidentified products. These products result from the reaction of unreacted alcohol with the acid produced when the reaction is performed at these higher temperatures, and they were difficult to isolate and identify (entries 2 and 3, Table 1).

Under the previously established reaction conditions, the oxidation of benzyl alcohol was also carried out using different nickel salts such as NiCl_2 and $\text{Ni}(\text{CH}_3\text{COO})_2 \cdot 2\text{H}_2\text{O}$ instead of $\text{NiSO}_4 \cdot 6\text{H}_2\text{O}$ (entries 4 and 5, Table 1). It was noticed that the oxidation was quite slow and a considerably lower amount of benzoic acid was obtained. The differences in the yields obtained when the reactions were performed with the different nickel salts reflected their differences in solubility, i.e., a higher product yield was obtained with $\text{NiSO}_4 \cdot 6\text{H}_2\text{O}$ than with $\text{NiCl}_2 \cdot 2\text{H}_2\text{O}$ and $\text{Ni}(\text{CH}_3\text{COO})_2 \cdot 2\text{H}_2\text{O}$ because $\text{NiSO}_4 \cdot 6\text{H}_2\text{O}$ is more soluble in the reaction medium than the other salts.

On the other hand, a blank experiment was conducted in the absence of $\text{NiSO}_4 \cdot 6\text{H}_2\text{O}$, whereby the reaction did not proceed to completion and the acid was not detected (entry 6, Table 1). We separated the produced grey-green nickel oxide powder at the end of the reaction via filtration and washing with deionized water, recycled three times (entries 7, 8, and 9, Table 1) to produce nickel peroxide NPNPs, again with either excess $\text{K}_2\text{S}_2\text{O}_8$ in 1.0 M KOH or KBrO_3 in 1.0 M K_2CO_3 , and used this for further catalytic oxidation reactions of benzyl alcohol to the corresponding acid benzoic, giving 80%, 76%, and 60% yields, respectively.

Table 1. Optimization of the reaction conditions.

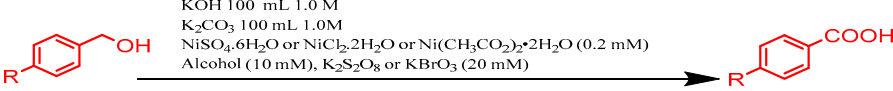
Entry	Co-Oxidant	Y (%)	TO	TOF (h ⁻¹)
1	K ₂ S ₂ O ₈	97	48.5	12.13
	KBrO ₃	75	36	9
2	K ₂ S ₂ O ₈	85	42.5	10.63
	KBrO ₃	60	30	7.5
3	K ₂ S ₂ O ₈	81	40.5	10.13
	KBrO ₃	63	31.5	7.9
4	K ₂ S ₂ O ₈	70	35	8.75
	KBrO ₃	54	27	6.75
5	K ₂ S ₂ O ₈	50	25	6.25
	KBrO ₃	50	25	6.25
6	K ₂ S ₂ O ₈	0	0	0
	KBrO ₃	0	0	0
7	K ₂ S ₂ O ₈	80	40	10
	KBrO ₃	70	35	8.75
8	K ₂ S ₂ O ₈	76	38	9.5
	KBrO ₃	55	27.5	6.88
9	K ₂ S ₂ O ₈	60	30	7.5
	KBrO ₃	40	20	5

Reaction conditions: All reactions were carried out at ambient temperature except for entries 2 and 3, which were carried out at 50 °C and 80 °C, respectively, and entries 4 and 5, where 0.2 mM of NiCl₂·H₂O or 0.2 mM of Ni(CH₃COO)₂·2H₂O was used instead of NiSO₄·6H₂O, respectively. Reaction time = 4 h; yield (Y) (%) = number of moles of produced acid × 100/number of moles of alcohol; turn over (TO) = number of moles of product/number of moles of catalyst; turn over frequency (TOF) = number of moles of product/number of moles of catalyst per hour.

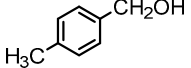
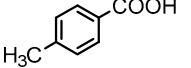
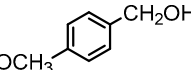
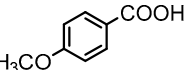
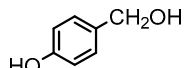
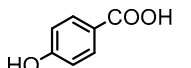
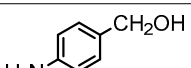
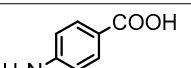
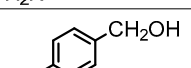
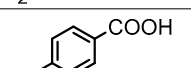
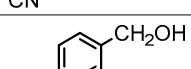
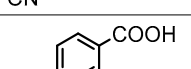
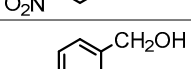
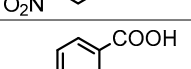
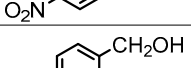
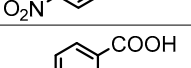
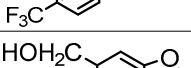
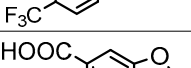
We noticed the yields obtained in the recycling of the catalyst were less than those obtained the first time, probably due to the loss of some of the catalyst during the reaction and also the loss of its active sites.

The effect of the *p*-derivatives on the yield of the acid was studied via the oxidation of some *p*-substituted electron-donating groups (*p*-CH₃, *p*-CH₃O, OH, and NH₂) and *p*-substituted electron-withdrawing groups (*p*-CHO, *p*-NO₂, *p*-CN, and *p*-CF₃). We found that the yields obtained with the electron-donating substituents (entries 10, 11, 12, and 13, Table 2) were higher than those obtained with the electron-withdrawing groups (entries 14, 15, 16, and 17, Table 2). The possible reason for these observations was the fact that the electron-donating groups activate the ring, thereby enhancing the oxidation of alcohol into the corresponding acid, while the electron-withdrawing groups deactivate the phenyl ring and in this way retard the reaction. The convincing evidence was the fact that the yield obtained with the first group was higher than that obtained with the latter.

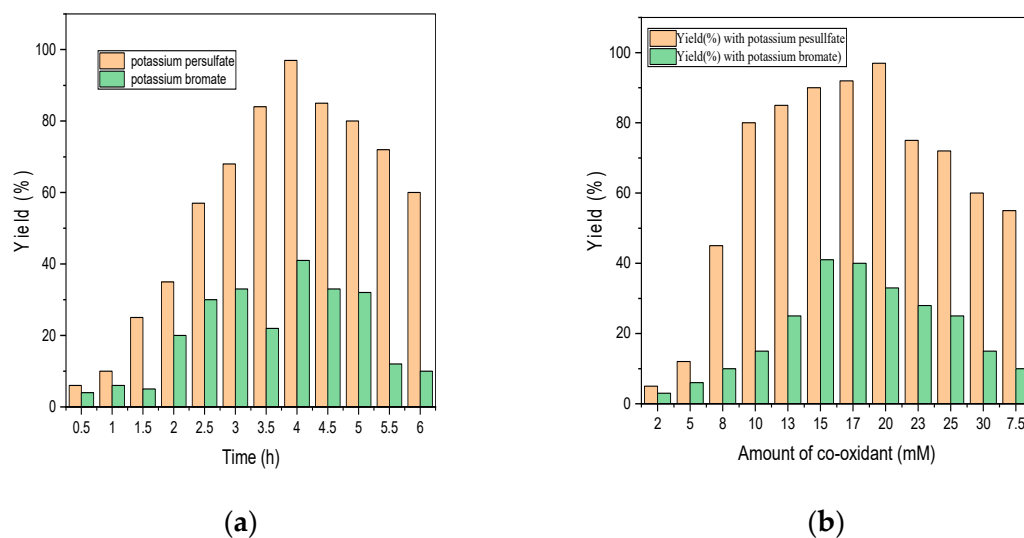
Table 2. The scope of the catalytic oxidation of benzyl alcohols to benzoic acids by NiSO₄·6H₂O/K₂S₂O₈.



(R = CH₃, OCH₃, OH, NH₂, CHO, CN, NO₂ and F₃C) and piperonyl alcohol

Entry	Substrate	Product	Co-Oxidant	Y (%)	TO	TOF (h ⁻¹)
10			K ₂ S ₂ O ₈	98	49	19.25
			KBrO ₃	70	35.5	8.6
11			K ₂ S ₂ O ₈	97	48.5	12.13
			KBrO ₃	63	31.5	7.5
12			K ₂ S ₂ O ₈	95	47.5	11.88
			KBrO ₃	65	32.5	7.9
13			K ₂ S ₂ O ₈	95	47.5	11.88
			KBrO ₃	66	33	8.25
14			K ₂ S ₂ O ₈	70	35.5	8.88
			KBrO ₃	40	20	5
15			K ₂ S ₂ O ₈	60	30	7.5
			KBrO ₃	30	15	3.75
16			K ₂ S ₂ O ₈	60	30	7.5
			KBrO ₃	30	15	3.75
17			K ₂ S ₂ O ₈	55	27.5	6.88
			KBrO ₃	25	12.5	3.13
18			K ₂ S ₂ O ₈	85	42.5	10.6
			KBrO ₃	50	25	6.25

However, we noticed that increasing the reaction time more than four hours (Figure 5a) and the amount of co-oxidants (K₂S₂O₈ and KBrO₃) more than 20 mM (Figure 5b) did not improve the yield.

**Figure 5.** (a) The time (h) against the yield (%) and (b) the amount of co-oxidant against the yield (%).

The reaction was self-indicating, whereby the green color of the reaction mixture changed to black upon the addition of potassium persulfate due to the formation of nickel peroxide nanoparticles (NPNPs). This color disappeared gradually with the formation of the green nickel oxide and completely disappeared when the potassium persulfate was consumed in the oxidation of the substrate.

However, this catalytic oxidation reaction is considered to be green because the reaction is selective and catalytic (alcohol is converted mainly to acid), the solvent used (water) is eco-friendly, and the oxidation is carried out at ambient temperature. However, our results are comparable with some recently reported protocols [36,37] for the catalytic oxidation of benzyl alcohols. It appears to be superior to most previously reported approaches. In our protocol, the yields of the acids were higher, and the reactions were conducted at room temperature with shorter reaction times than those reported by Han [38]. Recently, benzyl alcohol was catalytically oxidized to benzoic acid by the photocatalyst NH₂-MIL-125 (Ti) MOF in ethylacetate as a solvent and with O₂ as co-oxidant. In our recipe, we used water as a solvent, which is environmentally better than ethyl acetate, for which the reaction is longer than ours [39]. The catalyst, Ni@C/TiO₂-Z, was hydrothermally prepared and used for the oxidation of benzyl alcohol to benzoic acid at 96% in ethylacetate as a solvent for 18 h (a longer reaction time than our protocol) [40].

Finally, this protocol did not use any toxic solvent or chemical and was selective (the only product is the acid, with water as the sole by-product).

2.5. Mechanism of the Catalysis

It is very meaningful to trace the reaction process of the oxidation of alcohol to benzoic acid (BzCOOH) to understand the mechanism based on time-dependent curves (the percentages of BzOH, BzCHO, and BzCOOH with the reaction times) (Figure 6).

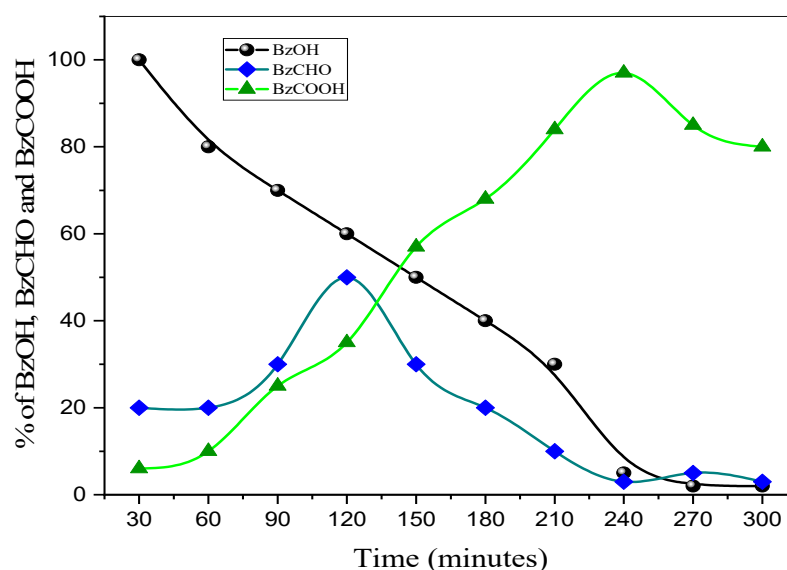


Figure 6. Time-dependent curves, showing the percentages of BzOH, BzCHO, and BzCOOH and the times in minutes.

Firstly, benzaldehyde was produced as a mid-product with consumption of half the amount of NiO₂ (first step) (Equation (2)):



Next, in the second step, the produced amount of benzaldehyde (BzCHO) decreased gradually due to its conversion to benzoic acid (BzCOOH) (Equation (3)):

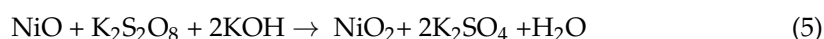


In this second step, the other half of the NiO_2 was completely consumed; thus, stoichiometrically, two moles of NiO_2 reacted with one of benzyl alcohol (BzOH) to produce one mole of benzoic acid (BzCOOH) according to the following Equation (4).

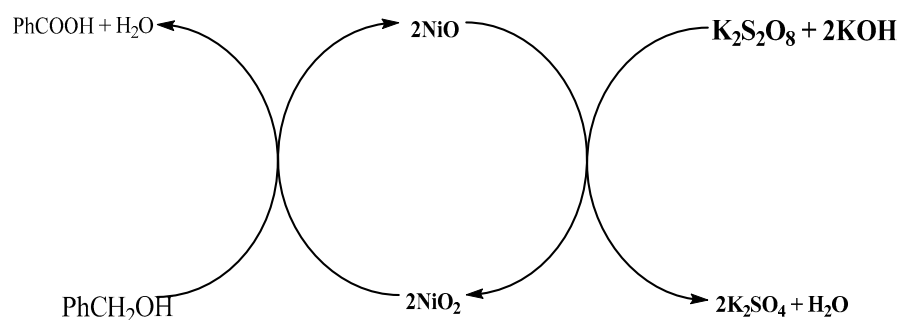


For this reason, the amount of the co-oxidant ($\text{K}_2\text{S}_2\text{O}_8$) was in two-fold excess of the benzyl alcohol (BzOH) and fifty-fold excess of the nickel salt. This means two oxidation steps occur at the same rate; therefore, we expect that the oxidation of benzyl alcohol (BzOH) to benzaldehyde (BzCHO) represents the rate-determining step [39].

However, the mechanism of this reaction occurred through the hydrogen abstraction mechanism, where benzyl alcohol (BzOH) coordinated to the nickel peroxide to form an unstable intermediate complex, which underwent intramolecular arrangement to produce the corresponding benzaldehyde (BzCHO) and nickel oxide. The produced nickel oxide reacted again with the excess of $\text{K}_2\text{S}_2\text{O}_8$ to produce nickel peroxide (Equation (5)):



This product similarly reacted with the produced benzaldehyde (BzCHO) to produce benzoic acid (BzCOOH). This catalytic cycle continued until the benzyl alcohol (BzOH) and benzaldehyde (BzCHO) were completely consumed (Scheme 2).



Scheme 2. Catalytic cycle of the oxidation of benzyl alcohol to benzoic acid.

3. Materials and Methods

All chemicals were purchased from Sigma-Aldrich (Berlin, Germany) ($\text{NiSO}_4 \cdot 6\text{H}_2\text{O}$, $\text{NiCl}_2 \cdot 2\text{H}_2\text{O}$, $\text{Ni}(\text{CH}_3\text{COO})_2 \cdot 2\text{H}_2\text{O}$, $\text{K}_2\text{S}_2\text{O}_8$, KOH , benzyl alcohol (BzOH), and *p*-substituted benzyl alcohols (R-BzOH; R = CH_3 , OCH_3 , OH , NH_2 , CHO , CN , NO_2 , and F_3C). The Fourier Transmission Infrared (FTIR) spectrum of NiO_2 was recorded through Alpha-Bruker FTIR spectrophotometer (model no. 200695, Berlin, Germany). The X-ray diffraction (XRD) pattern of NiO_2 with $\text{Cu K}\alpha$ radiation was obtained using PANalytical X'pert Pro X-ray diffractometer (DY 3190, Tokyo, Japan). Field Emission Scanning Electron Microscope (FESEM) Micrograph of NiO_2 was obtained by Carl Zeiss FESEM (SUPRA, 55VP, Berlin, Germany). Energy Dispersive X-ray (EDX) spectrum of NiO_2 was obtained by EDX detector of Oxford instruments (America) attached with FESEM. Transmission Electron Microscope (TEM) image of NiO_2 was taken by Jeol TEM (JEM-2100, Tokyo, Japan). ^1H NMR spectra were recorded on a Bruker DPX (600 MHz, London, UK).

3.1. Preparation of Nickel Peroxide Nanoparticles (NPNPs)

The nickel peroxide (NPNPs) were prepared using the co-precipitation method [24,25]. In a typical experiment, a solution of $\text{NiSO}_4 \cdot 6\text{H}_2\text{O}$ (13.15 g, 0.05 mol) in 75 mL of H_2O was added to the solution of $\text{K}_2\text{S}_2\text{O}_8$ (13.52 g, 0.05 mol) in 75 mL of H_2O with stirring. To this mixture, 150 mL of 2.0 M KOH (16.8 g, in 150 mL H_2O) was added in portions within one hour with continual stirring for a further 2 h. A black fine precipitate of nickel peroxide (NPNPs) was formed and collected by filtration, then thoroughly washed with deionized water and dried at 60°C (yield: 90%).

3.2. General Procedure for the Oxidation of Alcohol

Alcohol (10 mM) and $\text{NiSO}_4 \cdot 6\text{H}_2\text{O}$ (0.2 mM) were added to a 250 mL flat-bottomed flask containing 100 mL of 1.0 M KOH. The reaction mixture was stirred for the 10 min, $\text{K}_2\text{S}_2\text{O}_8$ (20 mM) was added in three portions, then the reaction mixture was stirred for three hours. The black color of the nickel peroxide appeared then gradually disappeared, then the reaction mixture was acidified with 10 mL of 5% HCl, extracted by diethylether (3×10 mL) to remove the unreacted alcohol, and filtered to collect the produced acid. The IR spectrum, melting point, and ^1H NMR results were measured where appropriate and compared with authentic samples. The analysis for the produced acids is listed below.

1. Benzoic acid

White solid; mp 121–122 °C (122 °C) [20]. IR: 3405–2103, 1682, 1610, 1572, 1463, 1432, 1333, 1282 cm^{-1} . ^1H NMR (400 MHz, CDCl_3): δ = 12.27 (br s, 1H, COOH), 8.43 (d, J = 7.1 Hz, 2H, Ar-H), 7.61 (t, J = 7.4 Hz, 1H, Ar-H), 7.47 (t, J = 7.8 Hz, 2H, Ar-H).

2. 4-Methylbenzoic acid

Pale yellow solid; mp 180–181.2 °C (180–182 °C) [20]. IR: 3400–2295, 1666, 1621, 1579, 1526, 1427, 1330, 1286 cm^{-1} . ^1H NMR (400 MHz, dmsO-d_6): δ = 12.73 (br s, 1H, COOH), 7.67 (d, J = 8.0 Hz, 2H, Ar-H), 7.71 (d, J = 8.0 Hz, 2H, Ar-H), 2.58 (s, 3 H, CH_3).

3. 4-Methoxybenzoic acid

Pale yellow solid; mp 181.6–184 °C (182–184 °C) [20]. IR (neat): 3310–2105, 1675, 1610, 1571, 1512, 1420, 1291, 1253, 1172, 1160, 1123, 1100, 1020 cm^{-1} . ^1H NMR (400 MHz, dmsO-d_6): δ = 12.60 (br s, 1H, COOH), 7.93 (d, J = 8.8 Hz, 2H, Ar-H), 7.05 (d, J = 8.8 Hz, 2H, Ar-H), 3.82 (s, 3H, CH_3).

4. 4-Chlorobenzoic acid

White solid; mp 238.0–239.0 °C (239–240 °C) [20]. IR: 3300–2200, 1678, 1591, 1574, 1492, 1423, 1400, 1320, 1305, 1176 cm^{-1} . ^1H NMR (400 MHz, dmsO-d_6): δ = 13.32 (br s, 1H, COOH), 7.78 (d, J = 8.8 Hz, 2H, Ar-H), 7.68 (d, J = 8.4 Hz, 2H, Ar-H).

5. 4-Nitrobenzoic acid

Pale yellow solid; mp 138–139 °C (139 °C) [20]. IR: 3405–2210, 1709, 1611, 1571, 1517, 1475, 1418, 1343 cm^{-1} . ^1H NMR (400 MHz, dmsO-d_6): δ = 13.60 (br s, 1H, COOH), 8.43 (d, J = 8.0 Hz, 2H, Ar-H), 8.38 (d, J = 8.0 Hz, 2H, Ar-H).

6. 4-Cyanobenzoic acid

Pale yellow solid; mp 221.0–222 °C (219–221 °C) [20]. IR (neat): 3410–2300, 2221, 1675, 1620, 1560, 1439, 1325, 1276, 1173, 1122, 1126, 1030 cm^{-1} . ^1H NMR (400 MHz, dmsO-d_6): δ = 13.60 (br s, 1H, COOH), 8.13 (d, J = 8.0 Hz, 2H, Ar-H), 8.03 (d, J = 8.4 Hz, 2H, Ar-H).

7. 4-Trifluoromethylbenzoic acid

White solid; mp; 220.2–222.2 °C (220–222 °C) [20]. IR (neat): 3410–2105, 1684, 1583, 1515, 1420, 1310, 1285, 1130, 1125, 1121, 1055, 1028 cm^{-1} . ^1H NMR (400 MHz, dmsO-d_6): δ = 13.54 (br s, 1H, COOH), 8.16 (d, J = 8.0 Hz, 2H, Ar-H), 7.89 (d, J = 8.0 Hz, 2H, Ar-H).

8. Piperonylic acid

Colorless needles; mp 224–226 °C (228–232 °C) [20]. IR (neat): 3100, 2900, 2850, 1620, 1540, 1455, 1410, 1230, 1153, 1110, 1113, 1015 cm^{-1} . ^1H NMR ^1H NMR (250 MHz, CDCl_3) 7.77 (s, 1H, COOH), 7.50 (dd, 1H, J = 8 and 2 Hz, Ar), 6.22 (d, 1H, J = 2 Hz, Ar).

4. Conclusions

We introduced a straightforward and efficient catalytic method for the conversion of benzyl alcohol and some para-substituted benzyl alcohols to their corresponding carboxylic acids using $\text{NiSO}_4 \cdot 6\text{H}_2\text{O}$ (0.2 mM)/ $\text{K}_2\text{S}_2\text{O}_8$ (20 mM) in 100 mL of 1.0 M KOH and $\text{NiSO}_4 \cdot 6\text{H}_2\text{O}$ (0.2 mM)/ KBrO_3 (20 mM) in 100 mL of 1.0 m K_2CO_3 . The advantages of this

catalytic process are the use of non-toxic and inexpensive materials; the mild reaction conditions; the simple, safe procedure; and the short reaction times. The yields and turnover are good. This protocol can be extended for the catalytic oxidation of other organic substrates such as aromatic amines and secondary alcohols, which is currently under investigation in our laboratory.

Author Contributions: Conceptualization, A.G.F.S.; methodology, M.M.A.H.S.; software, N.A.E.-G.; validation, N.A.E.-G.; writing—original draft, A.G.F.S.; writing—review and editing, T.A.Y., M.M.A.-K. and S.H.K. All authors have read and agreed to the published version of the manuscript.

Funding: This research was supported by the Deanship of Scientific Research at Imam Mohammed Ibn Saudi Islamic University through research group no. RG-21-09-80.

Data Availability Statement: Not applicable.

Conflicts of Interest: The authors declare no conflict of interest.

References

1. Urgoitia, G.; Maiztegi, A.; SanMartin, R.; Herrero, M.T.; Domínguez, E. Aerobic oxidation at benzylic positions catalyzed by a simple Pd(OAc)₂/bis-triazole system. *RSC Adv.* **2015**, *5*, 103210–103217. [[CrossRef](#)]
2. Fatiadi, A.J. The Classical Permanganate Ion: Still a Novel Oxidant in Organic Chemistry. *Synthesis* **1987**, *1987*, 85–127. [[CrossRef](#)]
3. Larock, R.C. *Comprehensive Organic Transformations*; McGraw-Hill: New York, NY, USA, 1989.
4. Hoover, J.M.; Ryland, B.L.; Stahl, S.S. Mechanism of copper (I)/TEMPO-catalyzed aerobic alcohol oxidation. *J. Am. Chem. Soc.* **2013**, *135*, 2357–2367. [[CrossRef](#)]
5. Silva, T.F.S.; Martins, L.M.D.R.S. Recent Advances in Copper Catalyzed Alcohol Oxidation in Homogeneous Medium. *Molecules* **2020**, *25*, 748. [[CrossRef](#)] [[PubMed](#)]
6. Lee, D.G.; Chen, T. The oxidation of alcohols by permanganate. A comparison with other high-valent transition-metal oxidants. *J. Org. Chem.* **1991**, *56*, 18, 5341–5345. [[CrossRef](#)]
7. Suga, T.; Kihara, K.; Matsuura, T. Oxidation of Alcohols with *t*-Butyl Chromate. II. The Oxidation of Primary Aromatic Alcohols. *Bull. Chem. Soc. Japan* **1964**, *38*, 1141–1144. [[CrossRef](#)]
8. Goswami, S.; Arnab, A. Guanidinium Chlorochromate, a New, Efficient, and Mild Oxidizing Agent for Benzylic and Other Alcohols to Carbonyl Compounds in Water and Organic Solvents. *Synth. Commun.* **2011**, *41*, 2500–2504. [[CrossRef](#)]
9. Corey, E.J.; Suggs, J.W. Pyridinium chlorochromate. An efficient reagent for oxidation of primary and secondary alcohols to carbonyl compounds. *Tetrahedron Lett.* **1975**, *16*, 2647–2650. [[CrossRef](#)]
10. Göksu, H.; Burhan, H.; Mustafafov, S.D.; Sen, F. Oxidation of Benzyl Alcohol Compounds in the Presence of Carbon Hybrid Supported Platinum Nanoparticles (Pt@CHs) in Oxygen Atmosphere. *Sci. Rep.* **2020**, *10*, 5439–5452. [[CrossRef](#)]
11. Chan-Thaw, C.E.; Savara, A.; Villa, A. Selective Benzyl Alcohol Oxidation over Pd Catalysts. *Catalysts* **2018**, *8*, 431. [[CrossRef](#)]
12. Ratnam, A.; Kumari, S.; Kumar, R.; Singh, U.P.; Ghosh, K. Selective oxidation of benzyl alcohol catalyzed by ruthenium (III) complexes derived from tridentate mer-ligands having phenolato donor. *J. Organomet. Chem.* **2019**, *905*, 120986. [[CrossRef](#)]
13. Arico, A.S.; Bruce, P.; Scrosati, B.; Tarascon, J.-M.; Van Schalkwijk, W. Nanostructured materials for advanced energy conversion and storage devices. *Nat. Mater.* **2005**, *4*, 366–377. [[CrossRef](#)]
14. Whitesides, G.M. Nanoscience, nanotechnology, and chemistry. *Small* **2005**, *1*, 172–179. [[CrossRef](#)]
15. Yu, B.; Meyyappan, M. Nanotechnology: Role in Emerging Nanoelectronics. *Solid State Electronics. Solid-State Electron.* **2006**, *50*, 536–544. [[CrossRef](#)]
16. Guo, Y.G.; Hu, J.S.; Wan, L.J. Nanostructured Materials for Electrochemical Energy Conversion and Storage Devices. *Adv. Mater.* **2008**, *20*, 2878–2887. [[CrossRef](#)]
17. Somorjai, G.A.; Park, J.Y. Colloid Science of Metal Nanoparticle Catalysts in 2D and 3D Structures. Challenges of Nucleation, Growth, Composition, Particle Shape, Size Control and Their Influence on Activity and Selectivity. *Top. Catal.* **2008**, *49*, 126–135. [[CrossRef](#)]
18. Khan, P.; Saeed, K.; Khan, I. Nanoparticles: Properties, applications and toxicities. *Arab. J. Chem.* **2019**, *12*, 908–931. [[CrossRef](#)]
19. Wang, M.; Liu, H.; Ma, J.; Luo, N.; Zhao, Z.; Wang, F. Sustainable Productions of Organic Acids and Their Derivatives from Biomass via Selective Oxidative Cleavage of C–C Bond. *ACS Catal.* **2018**, *8*, 2129–2165. [[CrossRef](#)]
20. Orouzadeh, N.; Baradaran, Z.; Sedrpoushan, A. An efficient heterogeneous Cu(I) complex for the catalytic oxidation of alcohols and sulfides: Synthesis, characterization, and investigation of the catalyst activity. *J. Coord. Chem.* **2021**, *74*, 2344–23664. [[CrossRef](#)]
21. Coronel, N.C.; da Silva, M.J.; Ferreira, S.O.; da Silva, R.C.; Natalino, R. K5PW11NiO39-catalyzed oxidation of benzyl alcohol with hydrogen peroxide. *Chemistryselect* **2019**, *4*, 302–310. [[CrossRef](#)]
22. Goerge, M.V.; Balachandran, K.S. Nickel Peroxide Oxidation of Organic Compounds. *Chem. Rev.* **1975**, *75*, 491–513. [[CrossRef](#)]
23. Weijlard, J. Oxidation of Organic Compounds with Nickel Peroxide. *J. Am. Chem. Soc.* **1945**, *67*, 1031–1032. [[CrossRef](#)]
24. Nakagawa, K.; Konaka, R.; Nakata, T. Oxidation with Nickel Peroxide. I. Oxidation of Alcohols. *J. Org. Chem.* **1962**, *27*, 1597–1601. [[CrossRef](#)]

25. Nakagawa, K.; Onoue, H.; Sugita, J. Oxidation with nickel peroxide. *Chem. Pharm. Bull.* **1964**, *12*, 1135–1138. [[CrossRef](#)]
26. Shoair, A.G.F.; Shanab, M.M.A.H.; Mahmoud, M.H.H. Electrochemical and Catalytic Properties of oxo-ruthenate(VI) in Aqueous Alkaline Medium. *Int. J. Electrochem. Sci.* **2021**, *16*, 210446. [[CrossRef](#)]
27. Kooti, M.; Jorfi, M. Synthesis and characterization of nanosize NiO₂ and NiO using TritonX-100. *Cent. Eur. J. Chem.* **2009**, *7*, 155–158. [[CrossRef](#)]
28. Teoh, L.G.; Li, K.-D. Synthesis and Characterization of NiO Nanoparticles by Sol–Gel Method. *Mater. Trans.* **2012**, *53*, 2135–2140. [[CrossRef](#)]
29. Li, G.J.; Kawi, S. Synthesis, characterization and sensing application of novel semiconductor oxides. *Talanta* **1998**, *45*, 759–766. [[CrossRef](#)]
30. Ichiyanagi, Y. Wakabayashi, N.; Yamazaki, J. Magnetic properties of NiO nanoparticles. *Phys. B* **2003**, 329–333, 862–863. [[CrossRef](#)]
31. Limberg, C.; Matthias Driess, M. Facile Access to an Active γ -NiOOH Electrocatalyst for Durable Water Oxidation Derived From an Intermetallic Nickel Germanide Precursor. *Angew. Chem. Int. Ed.* **2009**, *48*, 8107–8110. [[CrossRef](#)]
32. Al-Ghamdi, A.A.; Mahmouda, W.E.; Yaghmour, S.J.; Al-Marzouk, F.M. Structure and optical properties of nanocrystalline NiO thin film synthesized by sol–gel spin-coating method. *J. Alloys Compd.* **2009**, *486*, 9–13. [[CrossRef](#)]
33. Bobinihi, F.F.; Fayemi, O.E.; Onwudiwe, D.C. Synthesis, characterization, and cyclic voltammetry of nickel sulphide and nickel oxide nanoparticles obtained from Ni(II) dithiocarbamate. *Mater. Sci. Semicond. Process.* **2021**, *121*, 105315. [[CrossRef](#)]
34. Jyoti, K.; Baunthiyal, M.; Singh, A. Characterization of silver nanoparticles synthesized using *Urtica dioica* Linn. leaves and their synergistic effects with antibiotics. *J. Radiat. Res. Appl. Sci.* **2016**, *9*, 217–227. [[CrossRef](#)]
35. Seguin, L.; Amatucci, G.; Anne, M.; Chabre, Y.; Strobel, P.; Tarascon, M.; Vaughan, G. Structural study of NiO₂ and CoO₂ as end members of the lithiated compounds by in situ high resolution X-ray powder diffraction. *J. Power Sources* **1999**, *81–82*, 604–606. [[CrossRef](#)]
36. Bordoloi, K.; Kalita, G.D.; Das, P. Acceptorless dehydrogenation of alcohols to carboxylic acids by palladium nanoparticles supported on NiO: Delving into metal–support cooperation in catalysis. *Dalton Trans.* **2022**, *51*, 9922–9934. [[CrossRef](#)] [[PubMed](#)]
37. Shrikant, D.; Tambe, S.D.; Eun Jin Cho, E.J. Organophotocatalytic oxidation of alcohols to carboxylic acids. *Bull. Korean Chem. Soc.* **2022**, *43*, 1226–1230. [[CrossRef](#)]
38. Wang, H.; Wu, Z.; Yu, H.; Han, S.; Wei, Y. Highly efficient oxidation of alcohols to carboxylic acids using a polyoxometalate-supported chromium(III) catalyst and CO₂. *Green Chem.* **2020**, *22*, 3150–3154. [[CrossRef](#)]
39. Wei, X.-Z.; Dagnaw, F.W.; Liu, J.; Ma, L. Highly selective photocatalytic oxidation of alcohols under the application of novel metal organic frameworks (MOFs) based catalytic system. *J. Colloid Interface Sci.* **2023**, *629*, 136–143. [[CrossRef](#)]
40. Song, Z.; Liu, J.; Hu, Y.; Li, S.; Zhang, X.; Ma, L.; Chen, L.; Zhang, Q. Solvent-controlled selective photocatalytic oxidation of benzyl alcohol over Ni@C/TiO₂. *Catal. Commun.* **2023**, *176*, 106628. [[CrossRef](#)]

Disclaimer/Publisher’s Note: The statements, opinions and data contained in all publications are solely those of the individual author(s) and contributor(s) and not of MDPI and/or the editor(s). MDPI and/or the editor(s) disclaim responsibility for any injury to people or property resulting from any ideas, methods, instructions or products referred to in the content.